

Supplementary Information

The miRNA-212/132 family regulates both cardiac hypertrophy and cardiomyocyte autophagy

Ahmet Ucar, Shashi K. Gupta, Jan Fiedler, Erdem Erikci, Michal Kardasinski,
Sandor Batkai, Seema Dangwal, Regalla Kumarswamy, Claudia Bang,
Angelika Holzmann, Janet Remke, Massimiliano Caprio, Claudia Jentsch,
Stefan Engelhardt, Sabine Geisendorf, Carolina Glas, Thomas G. Hofmann,
Michelle Nessling, Karsten Richter, Mario Schiffer, Lucie Carrier, L. Christian Napp,
Johann Bauersachs, Kamal Chowdhury, and Thomas Thum

<u>Contents:</u>	<u>Page:</u>
Supplementary Figures S1-S14	2-15
Supplementary Table S1	16
Supplementary Table S2	17
Supplementary Table S3	18
Supplementary Methods	19-24
Supplementary References	25

Supplementary Figure S1

MiR-212 and miR-132 regulate hypertrophy in cardiomyocyte cell lines

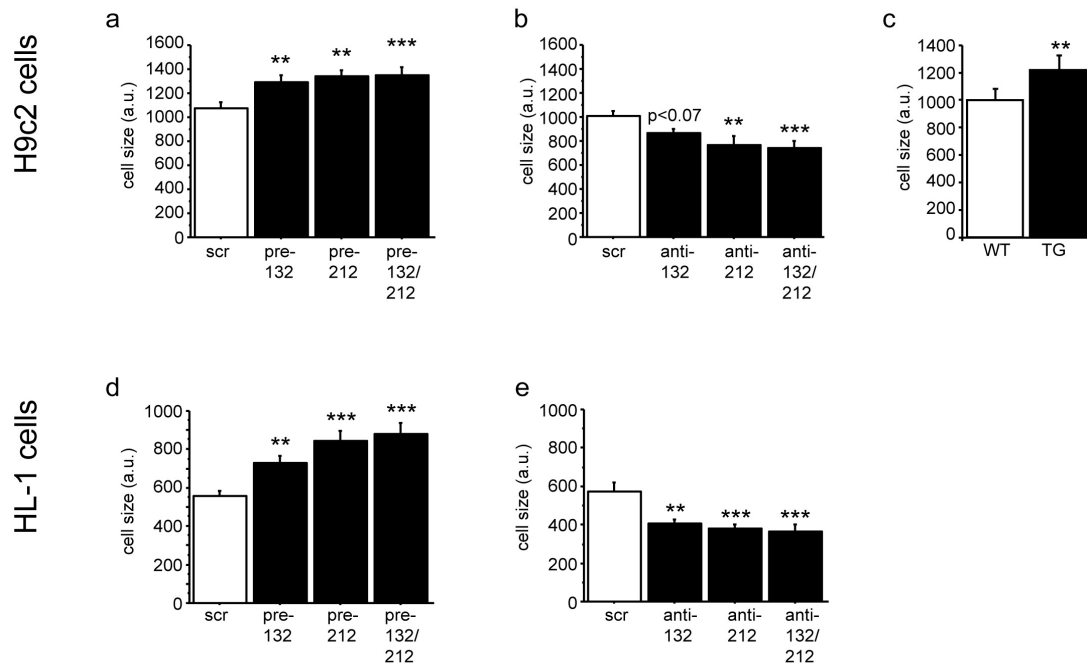


Figure S1. MiR-212 and miR-132 regulate hypertrophy in cardiomyocyte cell lines. Effects of overexpression of miR-212 and/or miR-132 precursors (pre-)(**a, d**) and silencing by inhibitors (anti-)(**b, e**) on size of H9c2 (**a, b**) and HL-1 (**d, e**) cells as compared to the effects of scrambled (scr) controls. (**c**) Cell size of wild-type (WT) and miR-212/132-overexpressing transgenic (TG) H9c2 cells. Values represent mean \pm SEM. (n=5-14); **:p<0.01; ***:p<0.005; a.u.: arbitrary unit.

Supplementary Figure S2

MiRNA family miR-212/132 suppresses apoptosis in H9c2 cells

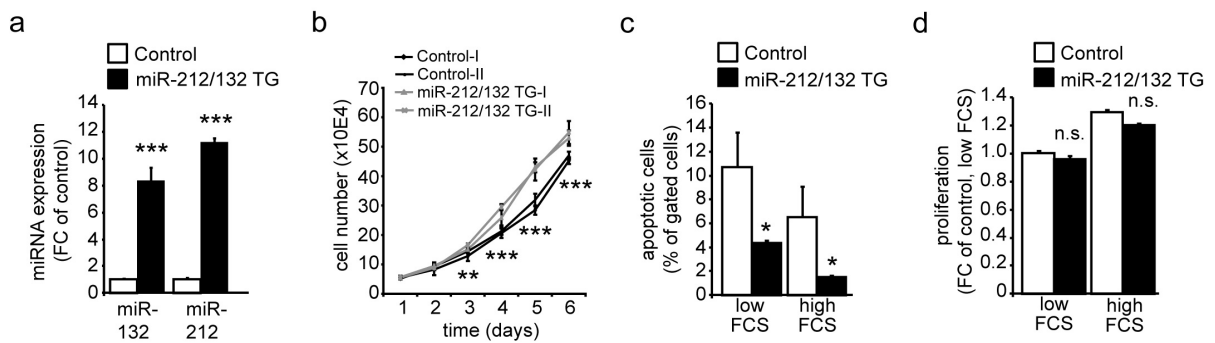


Figure S2. MiRNA family miR-212/132 suppresses apoptosis in H9c2 cells.

(a) Expression levels of miR-132 and miR-212 in transgenic miR-212/132-overexpressing (miR-212/132 TG) and control H9c2 cell lines. (n=3). (b) Time-dependent increase of cell number in two independent miR-212/132-overexpressing (TG-I and TG-II) and control (I and II) H9c2 cell lines. (n=6). (c, d) Number of apoptotic cells assessed by Annexin-V FACS analysis (c) and proliferation rate measured by WST assay (d) in the presence of high (10%) and low (1%) FCS in miR-212/132-overexpressing and control H9c2 cell lines. (n=6). All values represent mean \pm SEM in a, c, and d; and mean \pm SD in b. *:p<0.05; **:p<0.01; ***:p<0.005; ns: not significant; FC: fold-change.

Supplementary Figure S3

Overexpression of miR-212/132 family in the heart leads to cardiac hypertrophy

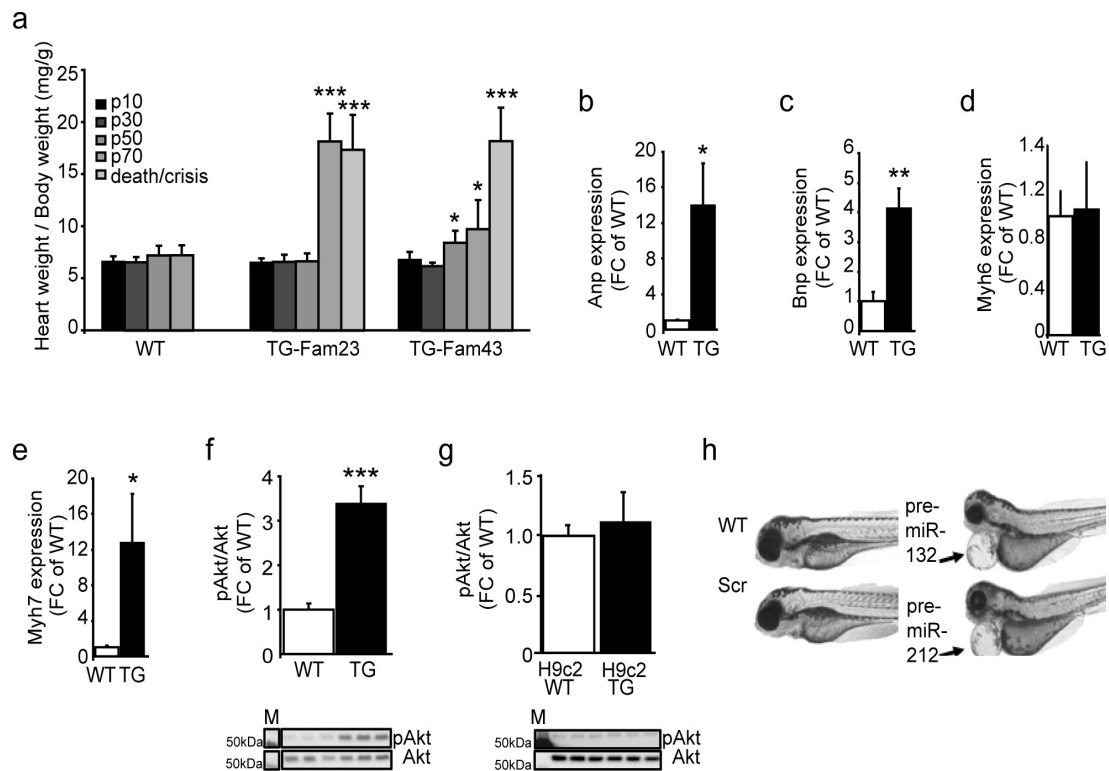


Figure S3. Overexpression of miR-212/132 family in the heart leads to cardiac hypertrophy.

(a) Heart-to-body weight ratios in wild-type (WT) and two independent cardiomyocyte-specific miR-212/132-overexpressing transgenic mouse lines (TG-Fam23 and TG-Fam43) between postnatal (p) day 10 and 70 as well as during death/crisis. Values represent mean \pm SEM. *: $p < 0.05$ versus p30 levels; ***: $p < 0.005$ versus p30 levels; (n=3-13). (b-f) Cardiac mRNA expression levels of Anp (b), Bnp (c), alpha-myosin heavy chain (Myh6; d), beta-myosin heavy chain (Myh7; e) and cardiac protein expression levels of p-Akt (relative to Akt; f) in cardiomyocyte-specific miR-212/132-overexpressing transgenic (TG) mice and their wild-type (WT) littermates. Values represent mean \pm SEM. * $p < 0.05$, ** $p < 0.01$, *** $p < 0.005$; (n=5-10). (g) pAkt/Akt ratios in wild-type (WT) and miR-212/132-overexpressing (TG) H9c2 cell lines (n=9). (h) Phenotype of wild type non-injected (WT), and scrambled miR (scr), pre-miR-132 or pre-miR-212 injected zebrafish embryos 48hrs post fertilization. The pre-miR-132 and pre-miR-212 injected embryos display a severe pericardial effusion, compared to scrambled injected or wild type control embryos (black arrows). M: Western blot marker; FC: Fold change.

Supplementary Figure S4

miR-212 and miR-132 repression does not effect proliferation, apoptosis or migratory behaviors of human cardiac fibroblasts

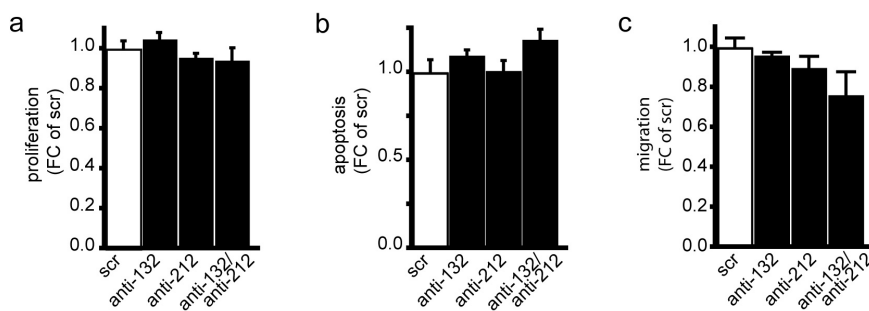


Figure S4. miR-212 and miR-132 repression does not effect proliferation, apoptosis or migratory behaviors of human cardiac fibroblasts.

Proliferation (a), apoptosis (b) and migration (c) of human cardiac fibroblasts 72 h post-transfection with scrambled control (scr), and anti-miR-212 and/or anti-miR-132. (n=6). All values represent mean \pm SEM.

Supplementary Figure S5

Absence of an overt vascular phenotype in miR-212/132 null mice

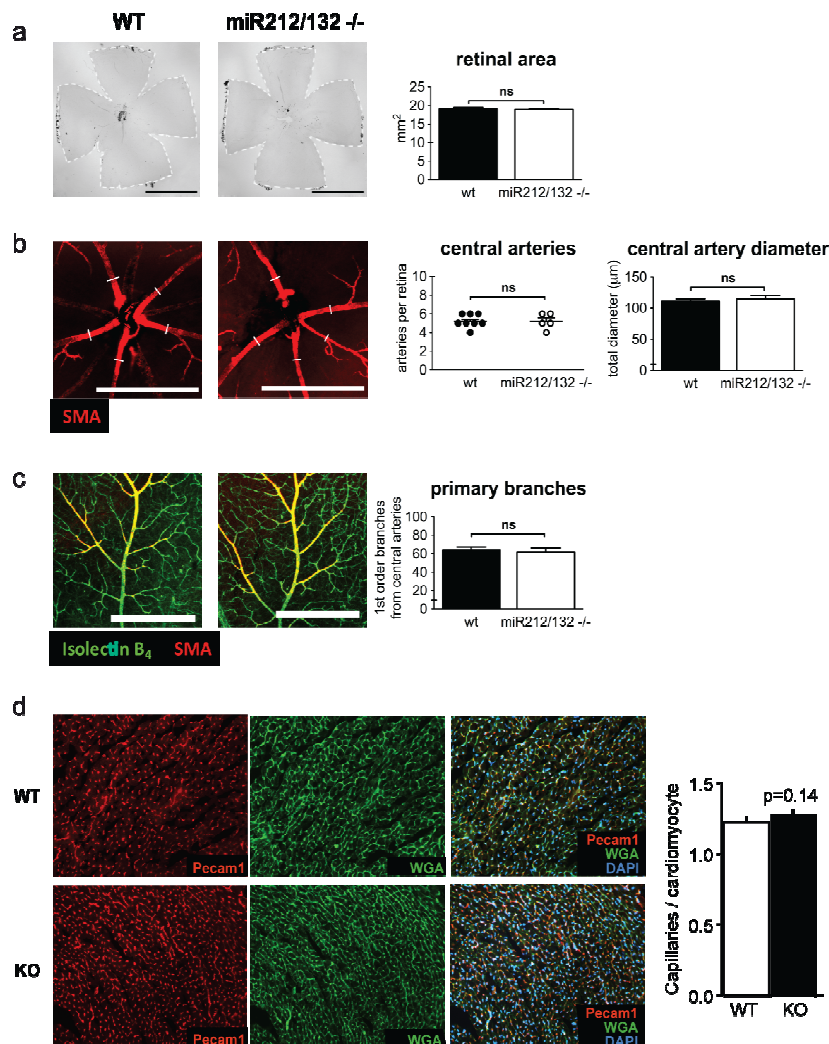


Figure S5. Absence of an overt vascular phenotype in miR-212/132 null mice.

The vascular system was studied in retinas of adult miR-212/132^{-/-} mice compared to wild-type (wt) littermates. Retinal area (**a**), number and total diameter of central retinal arteries originating from the optic nerve (**b**, measured at 200 µm distance from the optic nerve), and number of 1st order branches originating from central arteries (**c**, number per retina) were similar in miR-212/132^{-/-} mice and wild-type littermates. (n=5-8 retinas from at least 3 mice). (**d**) Staining of cardiac sections of wild-type (WT) and miR-212/132^{-/-} (KO) mice for Pecam1, wheat germ agglutinin and DAPI. Graph represents the number of capillaries per cardiomyocytes. (n=5). All values represent mean ± SEM. Scale bars represent 2 mm in **a**, 500 µm in **b** and **c**. ns: not significant.

Supplementary Figure S6

MiR-212/132 overexpression leads to FoxO3 downregulation and Mcip1.4 upregulation in cardiomyocytes

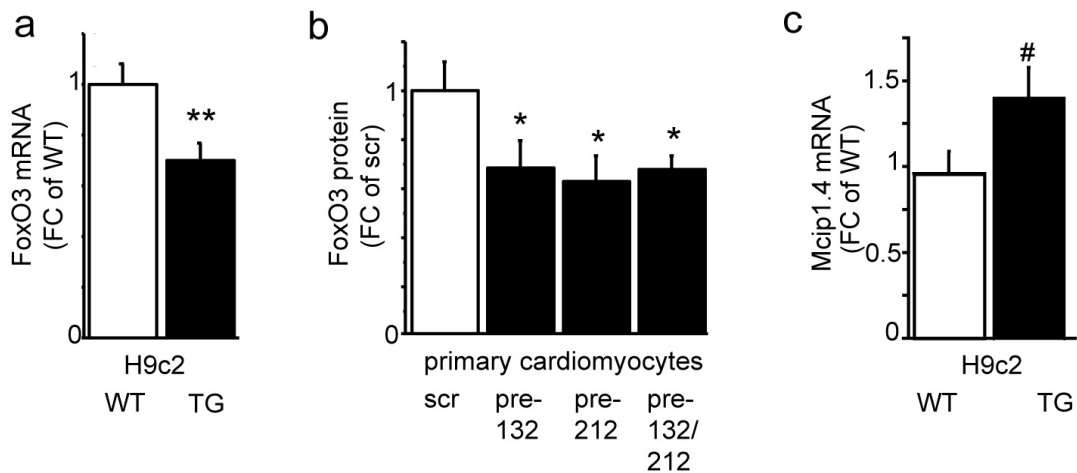


Figure S6. MiR-212/132 overexpression leads to FoxO3 downregulation and Mcip1.4 upregulation in cardiomyocytes.

(a) Expression of FoxO3 mRNA in wild-type (WT) and miR-212/132-overexpressing transgenic (TG) H9c2 cells. (b) FoxO3 protein levels in neonatal cardiomyocytes three days after transfection with scrambled controls (scr), miR-132, miR-212 or miR-132 and miR-212 precursor molecules. (c) Mcip1.4 mRNA levels in wild-type (WT) and miR-212/132-overexpressing transgenic (TG) H9c2 cells. FC: fold change. Values represent mean \pm SEM. * $p < 0.05$; ** $p < 0.01$; # $p = 0.052$ (n=4-7).

Supplementary Figure S7

miR-212/132 overexpression abrogates starvation-induced autophagy in primary cardiomyocytes

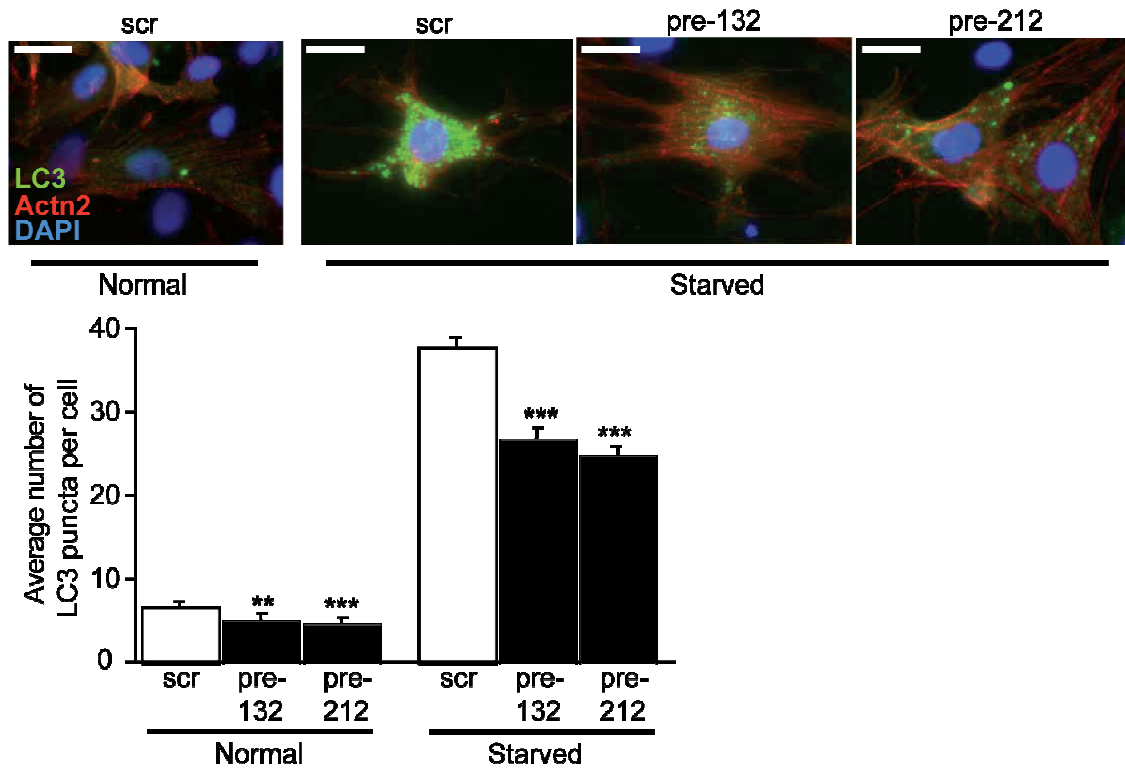


Figure S7. miR-212/132 overexpression abrogates starvation-induced autophagy in primary cardiomyocytes.

Average numbers of LC3-GFP puncta per cardiomyocytes were quantified in normal (DMEM + 10% FCS) media or starvation (glucose- and FCS-free) media after co-transfection with LC3-GFP expression construct together with scrambled control (Scr), pre-miR-212 or pre-miR-132. n=40-170 cardiomyocytes. All values represent mean \pm SEM. **p<0.01; ***p<0.005. Representative images are shown above the graph. Scale bars represent 10 μ m.

Supplementary Figure S8

Expression levels of the LC3-GFP fusion protein

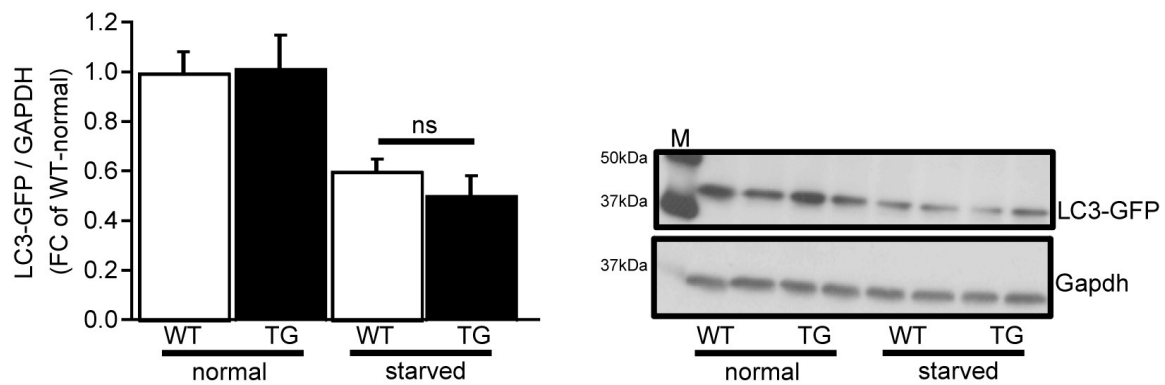


Figure S8. Expression levels of the LC3-GFP fusion protein.

Expression of the LC3-GFP fusion protein in wild-type (WT) and miR-212/132-overexpressing transgenic (TG) H9c2 cells in normal and starving (glucose and serum-free medium) cell culture conditions 24 hours post-transfection with LC3-GFP expression construct. Values represent mean \pm SEM. (n=4). FC: Fold change; ns: not significant; M: Western blot marker.

Supplementary Figure S9

Starvation leads to the downregulation of miR-212/132 expression in H9c2 cells

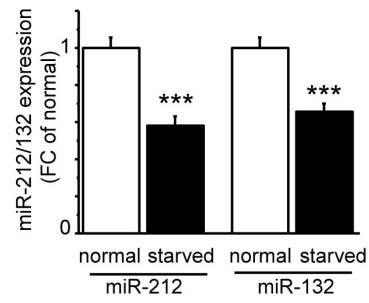


Figure S9. Starvation leads to the downregulation of miR-212/132 expression in H9c2 cells.

Expression levels of miR-212 and miR-132 in H9c2 cells 24h after normal conditions or serum/glucose deprivation. Values represent mean \pm SEM. *** $p < 0.005$; (n=9).

Supplementary Figure S10

Starvation-induced autophagy in the hearts of wild-type, miR-212/132 null and miR-212/132-overexpressing mice

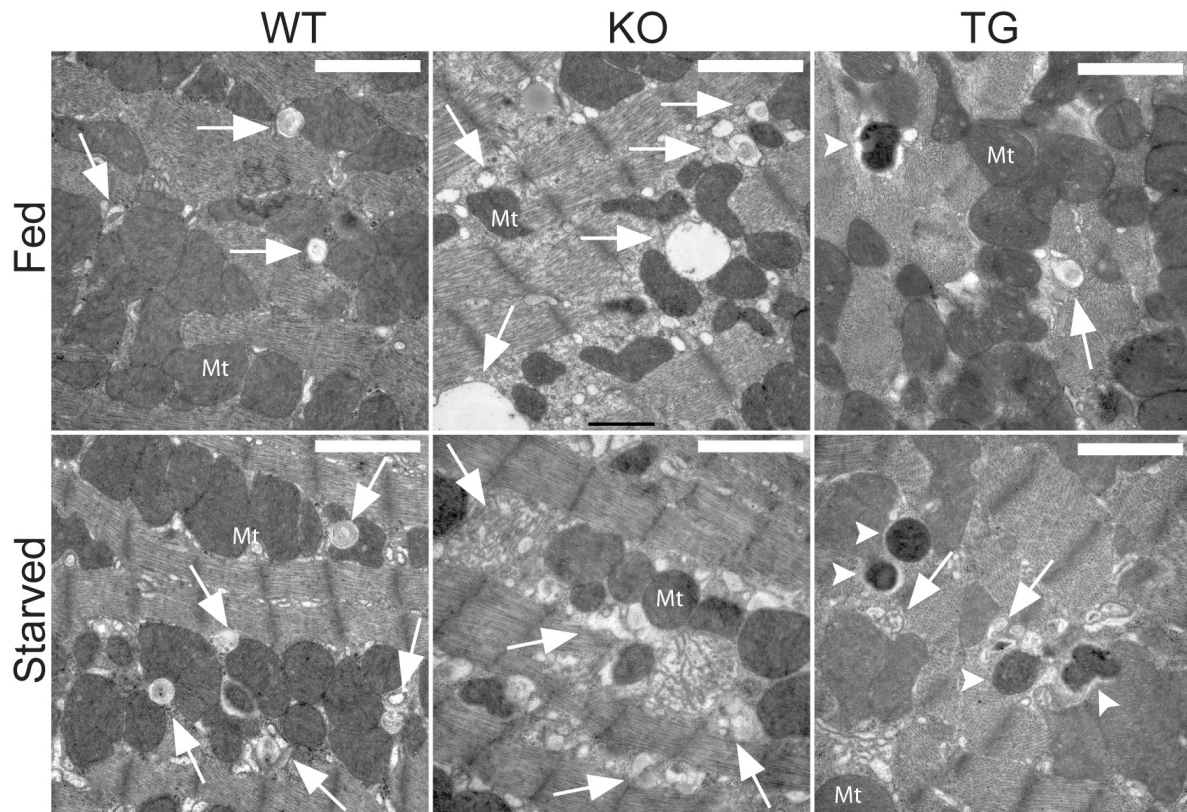


Figure S10. Starvation-induced autophagy in the hearts of wild-type, miR-212/132 null and miR-212/132-overexpressing mice.

Higher magnification electron micrographs of ultrathin heart sections presented in **Figure 6c** for the confirmation of autophagic vacuoles and autophagosomes within the cardiomyocytes of fed or starved wild-type (WT), miR-212/132 null (KO), and miR-212/132-overexpressing transgenic (TG) mice. Dark grey structures are mitochondria (Mt). The translucent structures (shown with arrows) contain either convoluted membrane structures or double layers of membranes indicative of autophagic vacuoles. The electron-dense black structures (shown with arrowheads) in cardiomyocytes of TG mice are autophagosomes / autolysosomes. Scale bars represent 1 μ m.

Supplementary Figure S11

Starvation leads to increased cardiac p62 levels *in vitro* and *in vivo*

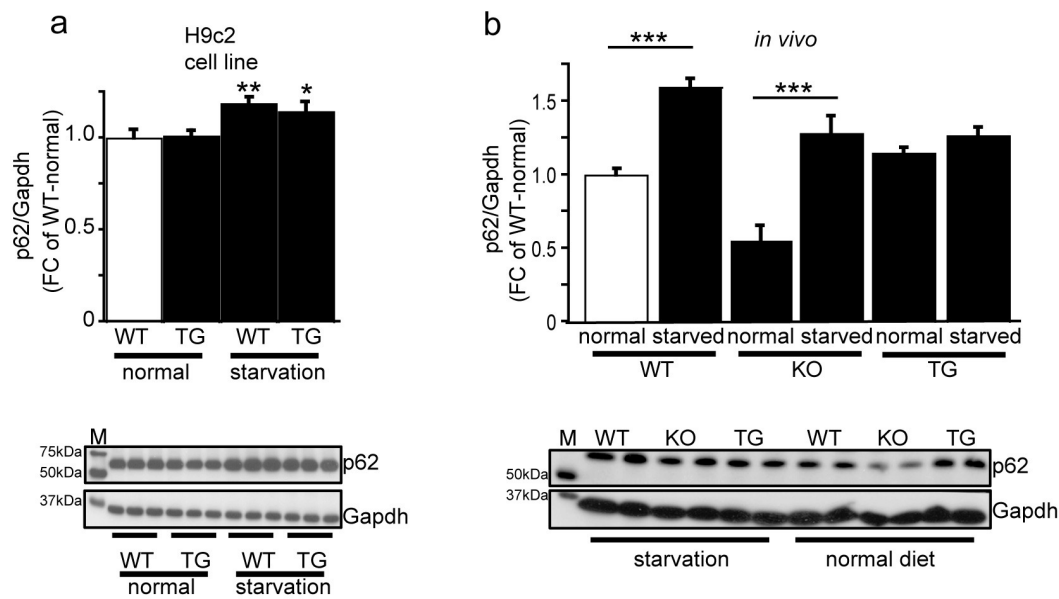


Figure S11. Starvation leads to increased cardiac p62 levels *in vitro* and *in vivo*.

(a) Expression of p62 protein in wild-type (WT) and miR-212/132-overexpressing transgenic (TG) H9c2 cells under normal and starving (glucose and serum-free medium) cell culture conditions for 24 hours (n=9). (b) Cardiac expression of p62 protein in wild-type (WT), miR-212/132 null (KO) and miR-212/132-overexpressing transgenic (TG) mice, which were either given ad libitum access to food (normal) or starved for a period of 31 hours (n=4). Representative western blot images are shown below the graphs. Values represent mean \pm SEM. *p<0.05; **p<0.01; ***p<0.05. M: Western blot marker.

Supplementary Figure S12

Reduced FoxO3 binding to LC3 promoter in miR-212/132-overexpressing H9c2 cells

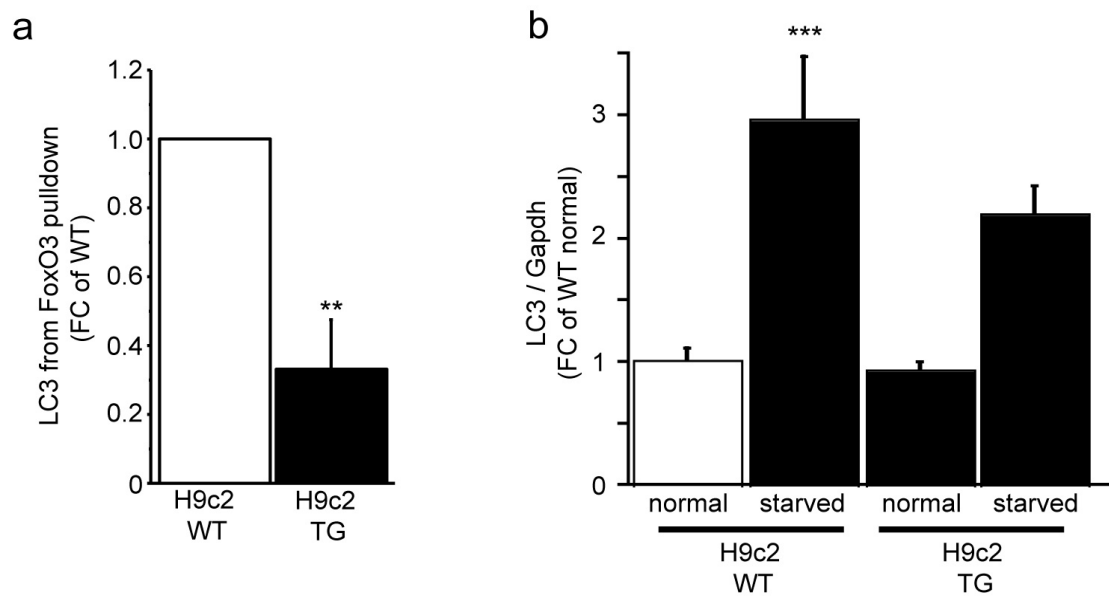


Figure S12. Reduced FoxO3 binding to LC3 promoter in miR-212/132-overexpressing H9c2 cells.

(a) LC3 promoter genomic sequence levels assessed by specific PCR reactions after the chromatin-immunoprecipitation by anti-FoxO3 antibodies from wild-type (WT) and miR-212/132-overexpressing (TG) H9c2 cells. (b) LC3 expression levels in wild-type (WT) and miR-212/132-overexpressing transgenic (TG) H9c2 cells under normal and starving (glucose and serum-free medium) cell culture conditions for 24 hours. Values represent mean \pm SEM. ** $p < 0.01$; *** $p < 0.005$; (n=3-6). FC: Fold change.

Supplementary Figure S13

Reduced cardiac miR-132 levels by antagomir treatment of left ventricular pressure-overloaded mice

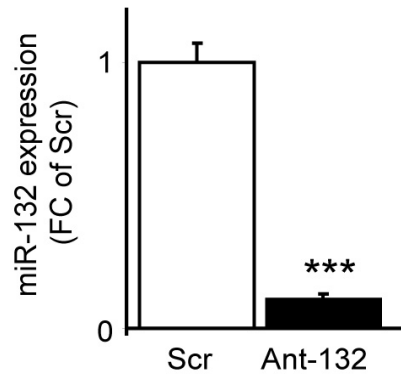


Figure S13. Reduced cardiac miR-132 levels by antagomir treatment of left ventricular pressure-overloaded mice.

Cardiac miR-132 expression in mice three weeks after the transaortic constriction and therapeutic injection of a scrambled antagomir (Scr) or an antagomir directed against miR-132 (Ant-132). Values represent mean \pm SEM. *** $p < 0.005$; (n=5-14). FC: Fold change.

Supplementary Figure S14

miR-1 expression is down-regulated by the overexpression of miR-212/132 family

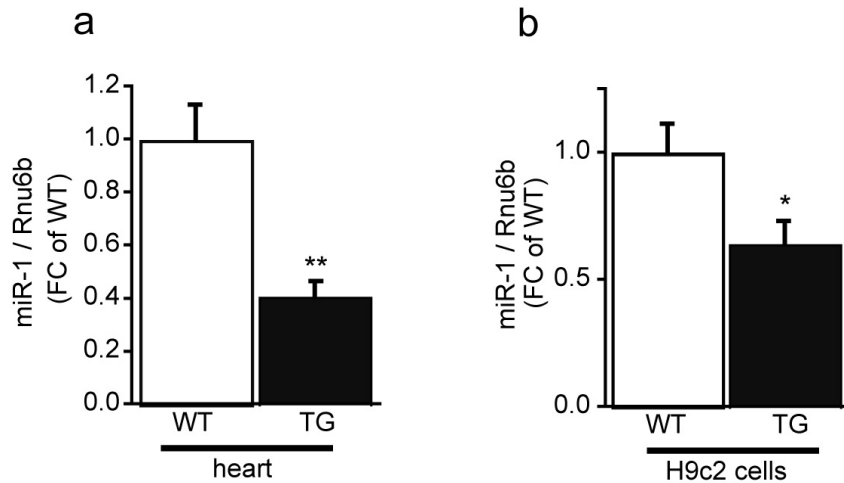


Figure S14. miR-1 expression is down-regulated by the overexpression of miR-212/132 family.

(a) miR-1 expression levels in hearts of wild-type (WT) and miR-212/132-overexpressing transgenic (TG) mice (n=5). (b) miR-1 expression levels in wild-type (WT) and miR-212/132-overexpressing transgenic (TG) H9c2 cell lines (n=8). Values represent mean \pm SEM. *p<0.05; **p<0.01. FC: Fold change.

Supplementary Table S1

Basic hemodynamic analysis of wild-type (WT) and cardiomyocyte-specific miR-212/132-overexpressing transgenic (TG) mice using pressure-volume catheter system

Hemodynamic parameters	WT (n=3)	TG (n=3)
HR (bpm)	506,05±36,03	487,00±54,35
Ped (mmHg)	2,05±5,42	6,00±3,30
EF (%)	70,43±9,71	38,36±3,65

HR: heart rate; Ped: left ventricular end diastolic pressure; EF: ejection fraction. All values represent mean ± S.E.M.; P values are only significant (<0.05) for EF between WT and TG.

Supplementary Table S2

Hemodynamic analysis of wild-type (WT) and miR-212/132 null (KO) mice using pressure-volume catheter system

Hemodynamic parameters	WT (n=8)	KO (n=6)
HR (bpm)	510,06±10,05	527,05±11,88
SV (μL)	16,43±0,68	16,38±0,54
Ves (μL)	16,45±1,47	14,26±1,59
Ved (μL)	31,26±1,98	27,58±2,60
Pes (mmHg)	87,38±2,66	86,73±3,05
Ped (mmHg)	3,83±0,39	2,62±1,06
dP/dt max (mmHg/s)	8689,95±424,21	9022,13±645,49
dP/dt min (mmHg/s)	-8753,19±451,06	-9063,34±416,60
SW (mmHgμL)	1232,15±54,49	1210,39±58,67
CO (μL/min)	8337,05±247,40	8622,58±270,95
EF (%)	54,65±1,91	61,86±4,57
Ea (mmHg/μL)	5,36±0,35	5,37±0,35
Tau (ms)	6,24±0,35	5,75±0,50

HR: heart rate; SV: stroke volume; Ves/Pes: left ventricular end systolic volume/pressure; Ved/Ped: left ventricular end diastolic volume/pressure; dP/dt: rate of rise of left ventricular pressure; SW: stroke work; CO: cardiac output; EF: ejection fraction; Ea: aortic elastance. All values represent mean ± S.E.M.; P values are all not significant between WT and KO.

Supplementary Table S3

Used oligonucleotide primer sequences

Gene	Species	Forward Reverse
Anp	Mouse	5'-CCTGTGTACAGTGCCGGTGTC-3' 5'-CCTAGAAGCACTGCCGTCTC-3'
Bnp	Mouse	5'-CTGAAGGTGCTGTCCCAGAT-3' 5'-GTTCTTTTGTGAGGCCTTGG-3'
α -MHC	Mouse	5'-GGTCCACATTCTTCAGGATTCTC-3' 5'-GCGTTCCTTCTCTGACTTTCG-3'
β -MHC	Mouse	5'-TCTCCTGCTGTTTCTTACTTGCT-3' 5'-CAGGCCTGTAGAAGAGCTGTACTC-3'
Gapdh	Mouse	5'-TTCACCACCATGGAGAAGGC-3' 5'-GGCATGGACTGTGGTCATGA-3'
Foxo3	Mouse	5'-CAAAGCTGGGTACCAGGCTG-3' 5'-TTCCACGGGTAAGGGCTTCA-3'
Foxo3	Rat	5'-GATGGTGCCTGTGTGCCCTAC-3' 5'-CCAAGAGCTCTTGCCAGTCCCTT-3'
LC3- promoter region (ChIP)	Rat	5'-GGCTGGACTTGAATTCAGAAA-3' 5'-ACTTGCTGTTCCAGGTGGTC-3'
Atrogin1	Mouse	5'-GCAAACACTGCCACATTCTCTC-3' 5'-CTTGAGGGGAAAGTGAGACG-3'
Atrogin1	Rat	5'-CCATCAGGAGAAGTGGATCTATGTT-3' 5'-GTTTCATGAAGTTCTTTTGGGCGATGC-3'
Mcip1	Mouse	5'-CTGCACAAGACCGAGTT-3' 5'-TGTTTGTCTGGGATTGG-3'
Mcip1	Rat	5'-AGCTCCCTGATTGCCTGTGT-3' 5'-TTTGGCCCTGGTCTCACTTT-3'
Lc3b	Mouse	5'-CGTCCTGGACAAGACCAAGT-3' 5'-ATTGCTGTCCCGAATGTCTC-3'
Ulk2	Mouse	5'-CAGCCCTGGATGAGATGTTT-3' 5'-GGATGGGTGACAGAACCAAG-3'
Atg12	Mouse	5'-GGCCTCGGAACAGTTGTTTA-3' 5'-CAGCACCGAAATGTCTCTGA-3'
Beclin1	Mouse	5'-GGCCAATAAGATGGGTCTGA-3' 5'-CACTGCCTCCAGTGTCTTCA-3'
Plk3c3	Mouse	5'-TGTCAGATGAGGAGGCTGTG-3' 5'-CCAGGCACGACGTAACCTTCT-3'
Bnip3	Mouse	5'-GAACTGCACTTCAGCAATGG-3' 5'-ATTTTCAGCTCTGTTGGTATC-3'
Atg5	Mouse	5'-GACAAAGATGTGCTTCGAGATGTG-3' 5'-ATAATGCCATTCAGGGGTGTGC-3'

Supplementary Methods

Retinal angiogenesis assay

Retina preparation and immunofluorescence were performed as previously described⁴⁸. In brief, whole eyes were fixed in 4% paraformaldehyde (PFA). Retinas were dissected, postfixed with PFA and blocked for 24 hours with PBS/BSA 1%/0.5% Triton X-100. After incubation with antibodies diluted in PBS/0.5%/0.25% Triton X-100 retinas were rinsed in PBS and mounted on a glass slide with coverslips using polyvinyl alcohol mounting medium (DAKO). The following reagents were used: Isolectin-B4-FITC (Vector, 1:100), anti-SMA-Cy3 (Sigma-Aldrich, 1:100). Stained retinas were analyzed with a fluorescence microscope (Zeiss Axiovert) using Axiovision software (Zeiss, Goettingen).

Zebrafish studies and miRNA injections

Wildtype (strain AB) were grown and mated at 28.5°C and embryos were kept and handled in standard E3 solution (5 mM NaCl, 0.17 mM KCl, 0.33 mM CaCl₂, 0.33 mM MgSO₄, 10⁻⁵ % methylene blue) buffered with 2 mM HEPES (Sigma-Aldrich, St. Louis, MO) as previously described⁴⁹. Using the Nanoject II injection device (Drummond Scientific, Broomall, PA), miR-132, miR-212 and scrambled controls were injected into one to four-cell stage fertilized embryos at 5μM final concentration in 4.6 nl injection buffer (20 mM Hepes, 200 mM KCl and 0.01% phenol red). Photographs were taken on a SMZ-U dissecting microscope (Nikon) and processed using Photoshop 3.0 (Adobe).

miRNA target prediction and validation

For the *in silico* screen of potential miRNA targets, miRNA databases and target prediction tools Miranda (<http://www.microrna.org/microrna/home.do>), PicTar (<http://pictar.mdc-berlin.de/>) and TargetScan (<http://www.target-scan.org>) were used. For validation of putative targets we used luciferase reporter assays. The 3'UTR sequence bearing seed region for miR-132/212 was cloned into SpeI and HindIII cloning site of a pMIR-REPORT vector (Ambion). We also generated clones with mutated miR-212 and miR-132 binding sites within the same 3'UTR sequence using a site-directed mutagenesis kit (Agilent Technologies). The cloned constructs were cotransfected with miRNAs of interest (Ambion) and β -galactosidase control plasmid (Promega) into HEK293 reporter cells seeded in 48-well plates using Lipofectamine 2000 (Invitrogen). In each case, 10 ng plasmid DNA and 100 nM miRNA were used. Cells were incubated for 24 h before luciferase and β -galactosidase activity was measured using the Luciferase Assay System (Promega) and Beta-Galactosidase Assay system (Promega) kits on a multi-plate reader (Biotek, Synergy HT) according to the manufacturers' instructions.

LC3:mCherry transfection and quantitation of autophagosomes

The expression construct for the LC3:mCherry fusion protein was kindly provided by Dr. Nathan Brady. Transgenic H9c2 cell lines were seeded on coverslips and after 80% confluence they were transfected with LC3:mCherry expression construct using Lipofectamine 2000 (Invitrogen) according to manufacturer's protocol. The transfection efficiency was kept between 10-20% in order to visualize single transfected cells afterwards. For the starvation groups, 12 hours after transfection, the medium

(DMEM+10%FCS) was replaced with DMEM only. After 24 hours culturing in DMEM, the medium is replaced with DMEM without glucose (GIBCO) and kept for additional 24 hours before fixation. For the 'full medium' groups, the medium changes are done exactly at the same times as above but always with DMEM+10% FCS. After treatments, the cells were fixed with 4% PFA, counterstained with Hoechst and mounted. The images of transfected cells were taken using a confocal laser scanning microscope (FluoView 1000; Olympus) with a 60x oil objective using the sequential scanning mode. Collected images were analyzed using ImageJ software with a special macro designed for the quantification of LC3 puncta in fluorescent images.

Transmission electron microscopy analyses

Transgenic H9c2 cell lines were seeded on 10-cm plates and first grown in DMEM+10% FCS till 90% confluency. Afterwards, for the 'starvation' groups, they were further cultured in DMEM only for 24 hours and then in DMEM without glucose for an additional 24 hrs. For the 'full medium' groups, the medium changes are done exactly at the same times but always with DMEM+10% FCS with glucose. At the end of these treatments, the cells were fixed with 2% glutaraldehyde (EM-grade, Polysciences Germany) buffered in 150 mM Na-cacodylate pH 7.2. The culture medium was directly replaced by the fixative, followed by two changes for fresh fixative and fixation over night at 4°C. After wash in buffer, the fixed cells were scraped off, centrifuged, the pellets post-fixed in buffered 1% Osmiumtetroxide (1h/ 4°C) and embedded in low-melting agarose. Osmium-fixation was stopped with 67% ethanol and followed by en-bloc fixation with 1% uranyl-acetate. After total dehydration through graded steps of

ethanol and propylene oxide, samples were embedded in epoxy-resin. Ultrathin sections were prepared at nominal thickness of 60 nm, contrasted by uranyl and lead and observed with an EM 912 (Carl Zeiss NTS, Germany). Micrographs were recorded on image plates and scanned at 17.5 μm resolution (Ditabis, Germany). The quantifications of autophagic vacuoles were done independently by two different individuals with the criteria of observing the double-membrane and vacuole space or convoluted membrane structures inside the autophagic vacuoles.

For the ultra-structural analyses of heart samples of fed and starved mice, small biopsies were prepared using fresh scalpels. Tissue pieces smaller than 1 mm^3 were prepared and immediately submerged in phosphate-buffered aldehyde containing 2% formaldehyde and 2% glutaraldehyde (both EM-grade, Polysciences Germany) and stored for several days at 4°C until proceeding for resin embedding, including postfixation with osmium and uranyl en block. Ultrathin sections were prepared from the cured resin-blocks at nominal thickness of 60 nm (Ultracut UCT, Leica, Germany) contrasted by uranylacetate and Reynold's leadcitrate and observed with an EM 912 (Carl Zeiss NTS, Germany). Micrographs were recorded on image plates to be scanned at 17.5 μm resolution (Micron IP-scanner, Ditabis, Germany).

FACS-based method of autophagic quantitation

The expression construct for the LC3:GFP fusion protein was kindly provided by Dr. Nathan Brady. Stably transfected H9c2 cells were seeded in 12 well plates one day prior to transfection, which is done by using LC3:GFP construct and Lipofectamine 2000 (Invitrogen) according to manufacturer's protocol. Six hrs post transfection, medium was

changed with DMEM+10%FCS (full medium) and incubated for 24 hr. Afterwards, for control groups full medium was given and for starvation group medium was changed with DMEM (no glucose + no FCS) to induce autophagy. 24 hr later cells were harvested and captured on Canto BD for FACS analysis. FACS data was analyzed using FlowJo software.

LC3-GFP transduction and quantitation of autophagosomes

Primary cardiomyocytes were isolated from neonatal rats and seeded in 12-well plates. After 48 hours, cells were transfected with precursor miRNAs (100 nM) and Lipofectamine 2000 (Invitrogen) and then transduced with adenovirus (m.o.i. 8) for GFP-LC3 fusion protein. Medium change was done 5-6 hours later. Twenty-four hours later medium was changed to normal (DMEM plus 10% FCS) and starvation medium (glucose and serum-free DMEM). After 24 hours medium was removed, cells were washed with PBS and fixed with 4% PFA. Cells were permeabilized with 0.1% Triton X-100 and then incubated with primary antibody against alpha-actinin overnight. Next day cells were washed with PBS and incubated with an Alexa-594 labelled secondary antibody and DAPI for 30 minutes. Pictures were taken at 40X with Nikon-Ti eclipse and puncta calculation was done with Nikon NIS-elements software.

FoxO3-chromatin-immunoprecipitation (ChIP) assay

Chromatin immunoprecipitation for FoxO3 in H9c2 cells was performed with the MAGnify™ Chromatin Immunoprecipitation System (Invitrogen). In brief, 200,000 cells were used for formaldehyde crosslinking. Immunoprecipitation was carried out with 5 µg

FoxO3 antibody (sc-9813X, Santa Cruz) or control antibody (sc-2028, Santa Cruz). Subsequent RT-PCR analysis of immunoprecipitated chromatin was performed applying primers as depicted in Supplementary Table S3.

Supplementary References:

48. Napp LC *et al.* Extrinsic Notch Ligand Delta-Like 1 Regulates Tip Cell Selection and Vascular Branching Morphogenesis. *Circ Res.* **110**, 530-535 (2012).
49. Hentshel, D.M., *et al.* Rapid screening of glomerular slit diaphragm integrity in larval zebrafish. *Am J Physiol Renal Physiol.* **293**, F1746-F1750 (2007).